WHOLE-CORE VALIDATION OF THE SUPERPHENIX REACTOR USING WIMS11 AND AN INVESTIGATION INTO A HYBRID RZ-HEX SP3 CALCULATION ROUTE

Una Davies[1], Ben Lindley[2], Brendan Tollit[2], and Eugene Shwageraus[1]

[1]University of Cambridge
Department of Engineering
Trumpington Street
Cambridge CB2 1PZ

[2]Wood
5 Kings Point House
Poundbury
Dorchester DT1 3BW

ud215@cam.ac.uk, ben.lindley@woodplc.com, brendan.tollit@woodplc.com

ABSTRACT

The Superphénix SFR has been modelled using the new MERLIN flux solver module of the WIMS reactor physics code. The reactor was simulated for a range of calculation cases which investigated the neutronic effects of different temperatures and control rod insertions, for the purposes of validation against experimental data and verification against Serpent. The WIMS results were found to be in good agreement with the experimental data and the Serpent benchmark. Two different MERLIN models were constructed: a detailed hexagonal-Z geometry in 172 groups, and a hybrid method which used a simplified RZ model to condense the data used in the calculation into fewer groups before using the full hexagonal-Z geometry. This hybrid method was found to decrease the time taken for the calculations by a factor of five while retaining a good level of accuracy.

KEYWORDS: sodium-cooled fast reactor, SP3, superphenix

1. INTRODUCTION

Among the six Gen-IV systems chosen by the Generation-IV International Forum the Sodium-cooled Fast Reactor (SFR) has been referred to as the 'most researched', in part due to the extensive existing experience that is already available from a wide range of projects in a variety of different countries [1]. This makes the SFR a promising candidate for further development as a commercial Gen-IV system and motivates the validation and verification of nuclear design tools for use in modelling SFR systems [2].

The nuclear sector has extensive experience in modelling LWRs and there are well-tested capabilities which enable excellent accuracy at a reasonable computational cost. However, there are several substantial differences between SFRs and LWRs that mean some LWR modelling techniques may not be suitable for translation to SFR modelling. These include the smaller contribution of the Doppler effect and the more significant effects of sodium voiding and geometric distortions. At present there is no consensus in the reactor simulation community on how best to capture these effects in SFR modelling and there is a strong need for verification and validation of a variety of nuclear codes for SFR purposes.

The Horizon-2020 ESFR-SMART project was launched in September 2017 and aims to enhance the safety of future SFR designs through developing the analytical capabilities of the nuclear sector for SFR simulation [3]. As part of this goal the largest SFR constructed to date, the French Superphénix (SPX) reactor, has been selected for use as a new SFR validation case. The data available from the tests performed over the lifetime of SPX will support the project objective of calibrating computational tools for SFR safety assessment. A set of initial commissioning tests, first reported in 1990 [4], were chosen as the starting point for the static neutronics as part of Task 2.1.1 of the ESFR-SMART project. This task was led by the Paul Scherrer Institute (PSI), who also generated the Serpent results used for verification in this paper [5].

As part of this ESFR-SMART task, the deterministic reactor physics code WIMS [6] was used to model the SPX start-up tests. The first part of this paper presents the WIMS results from these benchmark calculations, while the second part details an investigation into a new hybrid flux solver method developed with the aim of reducing computational time while maintaining a reasonable level of accuracy.

2. METHODOLOGY

2.1. Description of the Superphénix (SPX) Reactor

The SPX reactor was a large 2990MW core comprising 358 fuel subassemblies with both axial and radial fertile blankets. The annular fuel pins contained a U-Pu mixed oxide fuel and boron carbide control rods were used (21 Control Shutdown Devices (CSD), 3 Diverse Shutdown Devices (DSD)). SPX included fuel pins with upper and lower gas and steel pin plenna, a spacer grid, and empty subassemblies filled with sodium (e.g. in the follower region allocated for the control rod insertion). All dimensions and material compositions have been taken from the original special issue published on the SPX start-up tests [4], as collated and refined by PSI in the course of the ESFR-SMART task [5].

The commissioning tests considered in this benchmark were performed during the period January 1986 – December 1986 and included criticality, control rod worths, and reactivity feedback coefficient measurements. The ESFR-SMART task has replicated these tests through a series of 13 experimental cases.

2.2. WIMS SFR-specific Calculation Route

The next major WIMS release (WIMS11) includes a new 3D whole-core flux solver module named MERLIN, which has specific relevance to SFR cases due to its new hexagonal modelling capabilities. MERLIN is a 3D flux solver that represents the angular variation using the SPN method and will be included in the next major commercial release of WIMS. Both diffusion and SP3 solutions can be specified and k-eigenvalue, source, or time dependent problems can be considered. MERLIN also solves conservation equations for delayed precursors, which may be coupled to the main transport equation for all problem types. A wide range of geometry configurations are available and include a capability for modelling hexagonal cores through the HEX option, as well as an RZ model. This makes MERLIN particularly well-suited for SFR applications. The MERLIN 3D geometry used in this work is shown in Fig. 1.

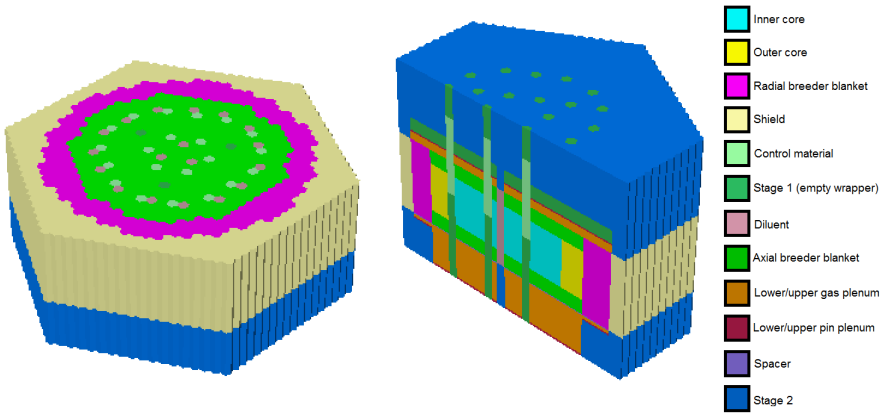

Figure 1: Full-core geometry shown cut horizontally through the upper axial blanket and vertically through the centre of the core.

The flexible modular nature of WIMS was utilised to tailor an SFR-specific calculation route as shown in Fig. 2a. The SPX subassemblies were modelled explicitly in 2D using different methods depending on the level of detail required. The fuel subassemblies were modelled using heterogeneous fine-group calculations performed in the WIMSECCO module followed by a 2D method of characteristics solver (CACTUS) to generate assembly-homogenised cross sections. The 2D supercell shown in Fig. 2b was used to correct the cross sections for the rodded regions with the super-homogenisation (SPH) method [7]. All other structural subassemblies were modelled by smearing their materials according to volume. These assembly-homogenised cross sections were then used in the 3D whole-core module MERLIN. The JEFF3.1.2 data library was used for all calculations.

The MERLIN 3D geometry shown in Fig. 1 was then used in the different calculation routes investigated here: HEX and hybrid.

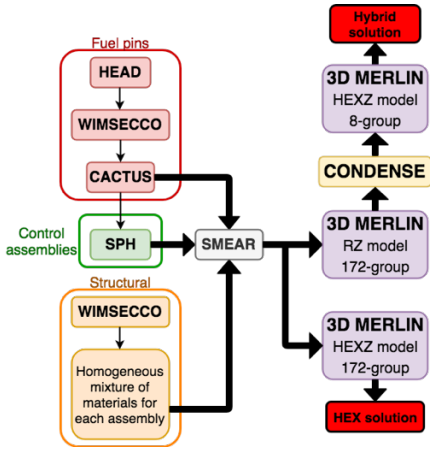

(a) WIMS modules used in route

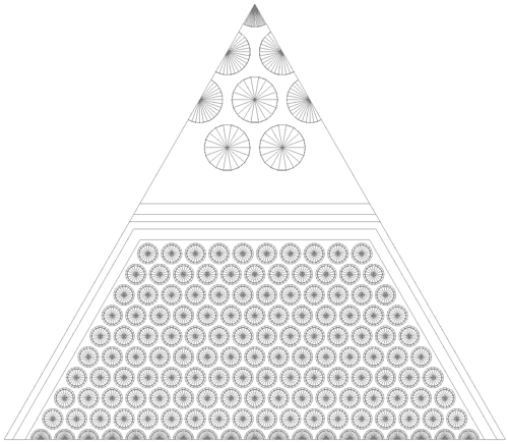

(b) 1/6 control rod with surrounding 1/2 fuel assembly

Figure 2: SPX WIMS calculation route and SPH supercell

2.2.1. HEX method

The MERLIN HEX method involves only the detailed 3D model of the SPX core in hexagonal-Z geometry shown in Fig.1. MERLIN then uses the assembly-homogenised cross sections calculated by the WIMSECCO (fuel and structural subassemblies) and SPH (regions containing control materials) modules for a designated number of energy groups. In this case, the number of groups for the HEX calculation was fixed at 172g.

2.2.2. Hybrid method

Further investigations were also conducted into a hybrid MERLIN RZ-HEX methodology which combines MERLIN radial-Z and hexagonal-Z solvers together. The RZ model used in this work may be seen in Fig. 3.

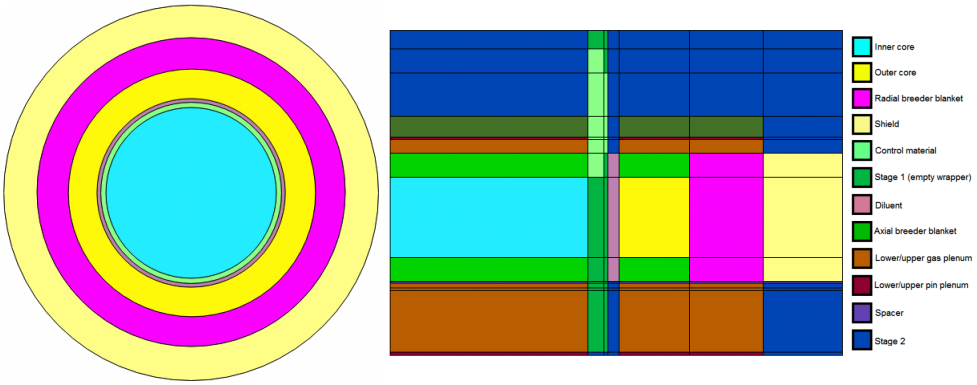

Figure 3: Radial (left) and axial (right) RZ SPX full-core simplified geometry in WIMS

The MERLIN module was used twice: first with the more approximate RZ model to provide a preliminary flux solution, and then with the detailed HEX model condensed to fewer energy groups. The detailed HEX model input used in the second step was exactly the same as the input used for the 172g HEX calculation. The aim of this investigation was to improve the runtime of the HEX calculation with a minimal loss of accuracy. The initial RZ approximate flux solution is performed in 172g, while the next detailed HEX calculation is condensed down to either 8g or 33g.

3. RESULTS

3.1. Benchmark Calculations

The initial calculation cases are set out in Table 1. The temperatures used to calculate the geometric parameters are given, as well as the temperatures at which the cross section libraries are specified. The final four cases include control rod insertions.

CASE ID	**CSD insertion (cm)**	**XS/GeometryTemperatures (K)**		
		Fissile	*Fertile*	*Structure*
1	0	453/453	453/453	453/453
2	0	673/673	673/673	673/673
3	0	1500/1500	900/900	673/673
4	0	300/300	300/300	300/300
5	0	300/453	300/453	300/453
6	0	300/673	300/673	300/673
7	0	600/673	600/673	600/673
8	0	900/673	900/673	900/673
9	0	600/673	600/673	300/673
10	40	300/673	300/673	300/673
11	40	600/673	600/673	600/673
12	40	673/673	673/673	673/673
13	100	453/453	453/453	453/453

Table 1: Superphénix calculation case descriptions

3.1.1. Initial criticality

The results for k-effective for each of the benchmark calculation cases is shown in Fig. 4. It can be seen that the agreement is generally good between the WIMS HEX method and the Serpent and experimental results, with a slight overestimation of rod worths in Case 13.

The average absolute difference between Serpent and MERLIN HEX is 137 pcm, which is deemed an acceptable discrepancy between a Monte Carlo calculation and a deterministic result.

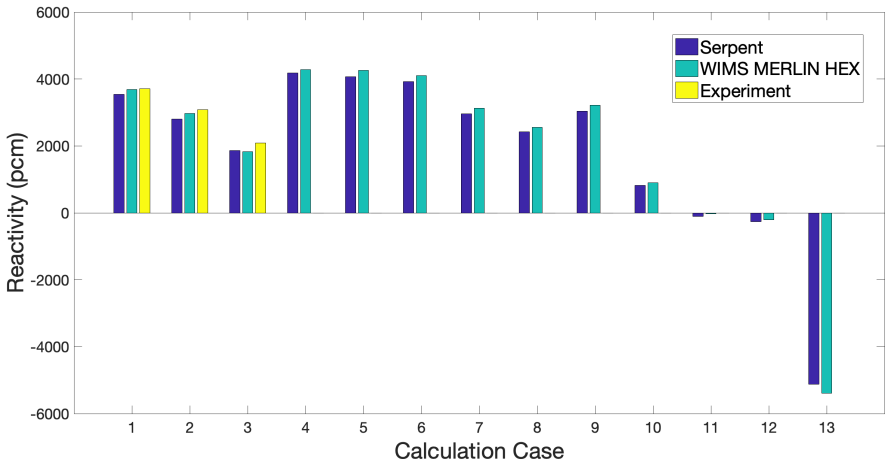

Figure 4: Results for the MERLIN HEX method compared with PSI Serpent results and, where available, experimental data

3.1.2. Doppler constants

The Doppler constants were calculated by taking cases at the same geometric temperature and changing the temperature at which the cross sections were evaluated. The control rods were kept in the parking position at the top of the fissile height for all cases. These results are presented in Table 2.

	Serpent (pcm)	**HEX (pcm)**
Case 6 - Case 7	−1381	−1406
Case 6 - Case 8	−1362	−1407
Case 6 - Case 9	−1265	−1275
Case 10 - Case 11	−1334	−1356

Table 2: Doppler constants for MERLIN HEX method compared with the PSI Serpent results

It can be seen that the WIMS results are within 45 pcm over the Serpent benchmark, which shows a good representation of the Doppler constants in the WIMS model.

3.1.3. Rod worths

The rod worths were evaluated by considering Cases 1 & 13. The same geometrical and cross section temperatures were used for both cases, the only difference being the insertion of the CSD control rods by 100 cm. The rod worth results are shown in Table 3.

	Serpent (pcm)	Experiment (pcm)	HEX (pcm)
Case 13 - Case 1	-8661	-8630	-9068

Table 3: Rod worths for MERLIN HEX method compared with the PSI Serpent results and experimental data

The WIMS calculation overestimates the control rod worth by around 400 pcm. One explanation for this could be that the CACTUS method of characteristics module is used in the SPH step, which introduces an inconsistency as the rest of the solution uses the SP3 method. In future work it would be better to use the MERLIN SP3 capabilities for the homogeneous solution as well.

3.1.4. Isothermal expansion coefficient

The isothermal expansion coefficient was calculated by considering Cases 1 & 2, corresponding to 453 K and 673 K (hot zero power). The expansion component has been evaluated by considering Cases 5 & 6, which use geometrical configurations at two different temperatures while keeping the cross section libraries at the same temperature. For all cases considered here the control rods are withdrawn to the top of the fissile height.

	Serpent	Experiment	HEX
Isothermal temperature coefficient (400-180°C) [pcm/°C]	3.34	2.87 ± 0.14	3.25
Expansion component *k* [pcm/°C]	0.70	0.74 ± 0.15	0.72
Doppler component K_D	1381	1180 ± 118	1406

Table 4: Isothermal expansion coefficients for MERLIN HEX method compared with the PSI Serpent results and experimental data

The WIMS model produces a drop in reactivity resulting from the transition of the core from Case 1 to Case 2 of -715 pcm, which compares well with the -733 pcm reactivity drop calculated by the Serpent benchmark. The value of the isothermal temperature coefficient is corresponding close to both the Serpent and the experimental result. The WIMS expansion coefficient and Doppler constant likewise agree closely with the Serpent benchmark and experimental results.

3.1.5. Power distribution

The radial power distribution of the core was mapped using the power in each subassembly. The maximum deviation observed between the WIMS MERLIN and Serpent results was -4.84 %, while the average absolute difference was 1.09%.

3.1.6. Reaction rates

The axial and radial reaction rates are shown in Figs. 5a - 5c. Figure 5a shows the axial profile of the U-235 fission rate calculated for the hot zero power core configuration, as compared with data from the original experiments [4] and the Serpent benchmark data [5]. Figure 5b & 5c show the radial profile of the U-238 and Pu-239 fission rates respectively at the fissile height. All profiles have been normalised to a maximum of 1, with arbitrary 3% error bars added onto the experimental value in keeping with the precedent set by PSI [5].

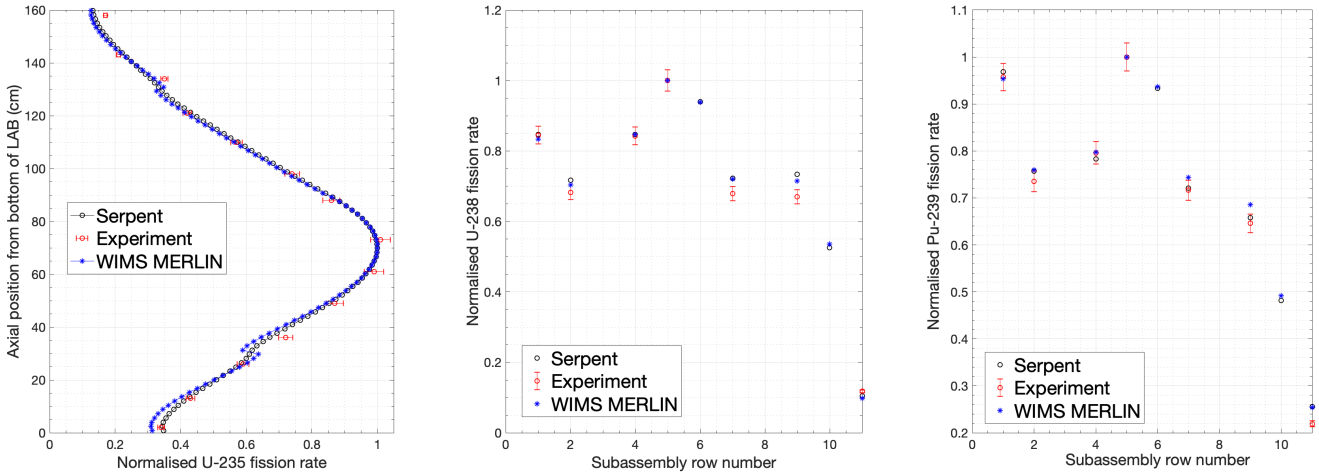

(a) **(b)** **(c)**

Figure 5: Reaction rates: axial profile of U-235, radial profile of U-238 in the fissile region, and radial profile of Pu-239 in the upper fertile blanket

There is an approximate agreement between the axial profiles of U-235 fission rates between WIMS MERLIN and the Serpent and experimental results over the core height, with some slight discrepancies at the boundaries between the top and bottom fertile axial blankets and the fissile fuel. The radial fission rates show a generally good agreement between the WIMS MERLIN results and the Serpent benchmark and experimental data for both the fissile and upper fertile blanket regions.

3.2. Comparison of HEX vs. Hybrid Methods

The hybrid method was then used for the same calculation cases from Table 1. All cases were run on a single thread core of a 28-core Intel Xeon CPU E5-2690 v4 2.60GHz cluster. The CPU runtime used for the modules was compared for each case and the average taken. Two different group structures were used: 8g and 33g. The Δk results between the new hybrid method and Serpent are shown in Fig. 6 and can be seen to be within 300 pcm. The MERLIN HEX method has the closest agreement with the Serpent results, followed by the 33g hybrid method, with the 8g hybrid method producing the greatest deviation from the benchmark.

The average differences between the two MERLIN hybrid methods and the Serpent benchmark

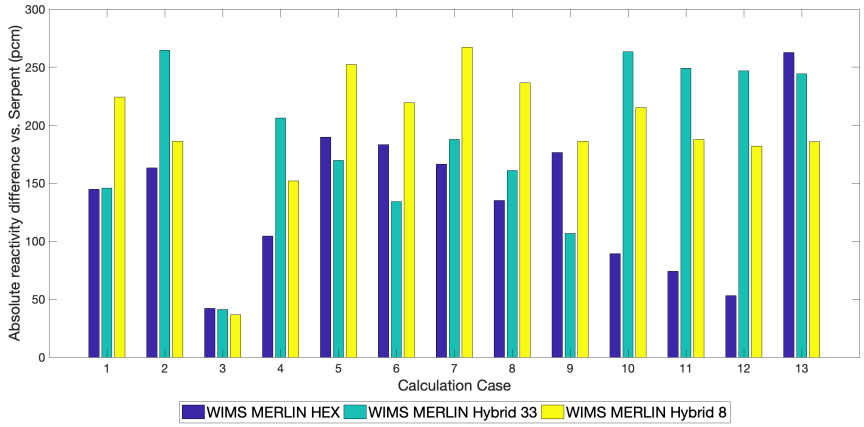

Figure 6: Results for the MERLIN HEX and hybrid methods, shown compared with PSI Serpent results and, where available, experimental data

are 195 and 186 pcm for the hybrid 8g and 33g methods respectively, compared to 137 pcm for the more detailed MERLIN HEX method. This small reduction in accuracy in the hybrid method may be acceptable if the computational cost savings are significant. Table 5 shows the difference in CPU time required to compute each of the results, taken as an average for all thirteen calculation cases performed here.

	Hybrid (8g)	**Hybrid (33g)**	**HEX (172g)**
Average solver computational time (CPU seconds)	473	1674	9767
Total route computational time (CPU seconds)	2216	3417	11479

Table 5: Isothermal expansion coefficients

The time taken for the MERLIN hybrid 8g module to complete its calculation is a factor of twenty times faster than the MERLIN HEX 172g module, while for the 33g hybrid module it is a factor of five times faster. When considering the total computation route calculation time the use of the WIMSECCO and SPH calculations is common to all methods, while the hybrid calculations also include the extra MERLIN RZ model step. This more representative comparison shows that the 8g and 33g hybrid methods are a factor of five and three times faster than the full MERLIN HEX method respectively.

4. CONCLUSIONS

The next WIMS release has been verified and validated using legacy data from the SPX reactor as part of the ESFR-SMART project. The sophisticated hexagonal geometry capabilities of the

new MERLIN flux solver have been used to model thirteen SPX calculation cases. The comprehensive results gathered for initial criticality, Doppler constants, rod worths, isothermal expansion coefficients, and reaction rates all show good agreement with both the experimental data and the Serpent benchmark results produced by PSI. Although there is some overestimation of the control rod worths by WIMS it is believed that this error arises due to a specific feature of the calculation route used in this work, which may be further investigated and removed by the next WIMS release. This work therefore illustrates the suitability of WIMS for SFR applications.

Investigations have also been conducted into a hybrid RZ-HEX calculation route within WIMS. This method uses a simplified RZ model of the hexagonal SFR core to condense the flux spectrum down to fewer groups before performing the calculation in the detailed hexagonal geometry. The aim of this investigation was to see whether the long calculation time required for the MERLIN HEX method could be reduced while retaining the accuracy of the model. The results presented in this paper show that, for a difference of 58 pcm between the MERLIN HEX and the MERLIN hybrid methods, the total computational time can be reduced by a factor of 5. This allows for considerable computational cost savings to be made with only a small reduction in accuracy.

ACKNOWLEDGEMENTS

This work has been prepared within EU Project ESFR-SMART which has received funding from the EURATOM Research and Training Programme 2014-2018 under the Grant Agreement No. 754501.

REFERENCES

[1] G. Locatelli, M. Mancini, and N. Todeschini. "Generation IV nuclear reactors: Current status and future prospects." *Energy Policy*, **volume 61**, pp. 1503–1520 (2013).

[2] K. Aoto, P. Dufour, Y. Hongyi, J. P. Glatz, Y.-i. Kim, Y. Ashurko, R. Hill, and N. Uto. "A summary of sodium-cooled fast reactor development." *Progress in Nuclear Energy*, **volume 77**, pp. 247–265 (2014).

[3] K. Mikityuk, E. Girardi, J. Krepel, E. Bubelis, E. Fridman, A. Rineiski, N. Girault, F. Payot, L. Buligins, G. Gerbeth, N. Chauvin, C. Latge, and J.-C. Garnier. "ESFR - SMART: new Horizon - 2020 project on SFR safety." In *International Conference on Fast Reactors and Related Fuel Cycles: Next Generation Nuclear Systems for Sustainable Developmen*. Yekaterinburg, Russia (2017).

[4] J. Gourdon, B. Mesnage, J. L. Voitellier, and M. Suescun. "An Overview of Superphénix Commissioning Tests." *Nuclear Science and Engineering*, **volume 106**(1), pp. 1–10 (1990).

[5] A. Ponomarev, A. Bednarova, and K. Mikityuk. "New Sodium Fast Reactor Neutronics Benchmark." In *PHYSOR 2018: Reactor Physics paving the way towards more efficient systems*. Cancun, Mexico (2018).

[6] B. Lindley, J. Hosking, P. Smith, D. Powney, B. Tollit, T. Newton, R. Perry, T. Ware, and P. Smith. "Current status of the reactor physics code WIMS and recent developments." *Annals of Nuclear Energy*, **volume 102**, pp. 148–157 (2017).

[7] A. Kavenoky. "The SPH homogenisation method." In *A Specialists' Meeting on Homogenization Methods in Reactor Physics, IAEA TECDOC-231* (1978).